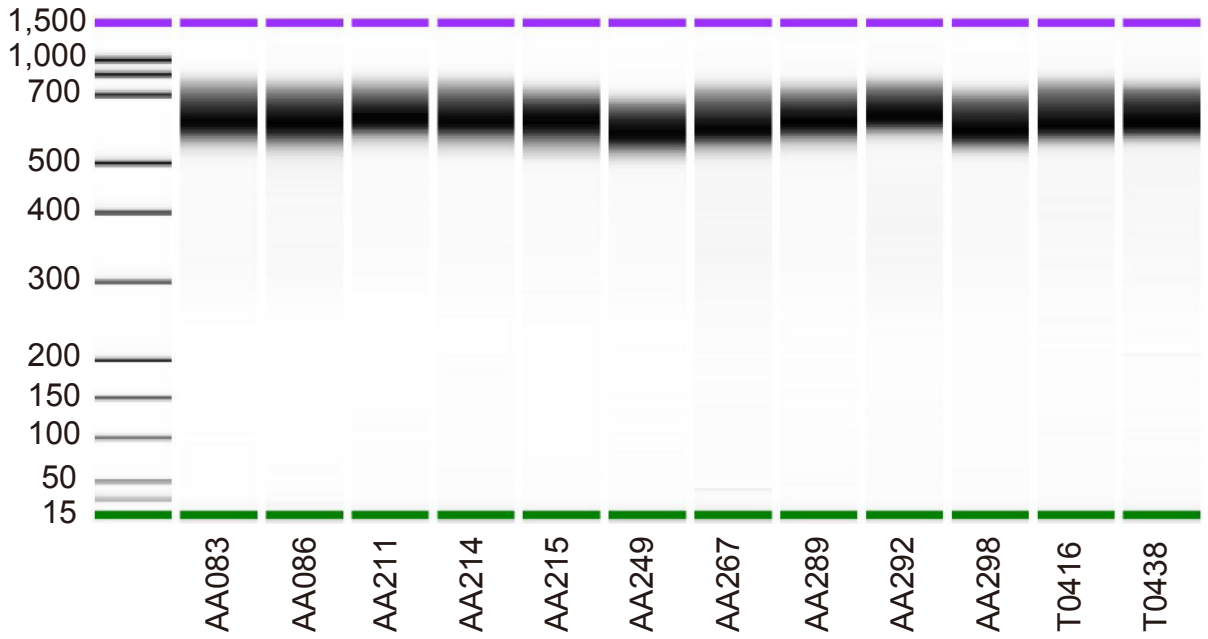

Supplementary Fig. 1. **Quantification and verification of genomic libraries.** We confirmed that the size of the libraries for pair end sequencing in the MHC region was 550-650 bp.

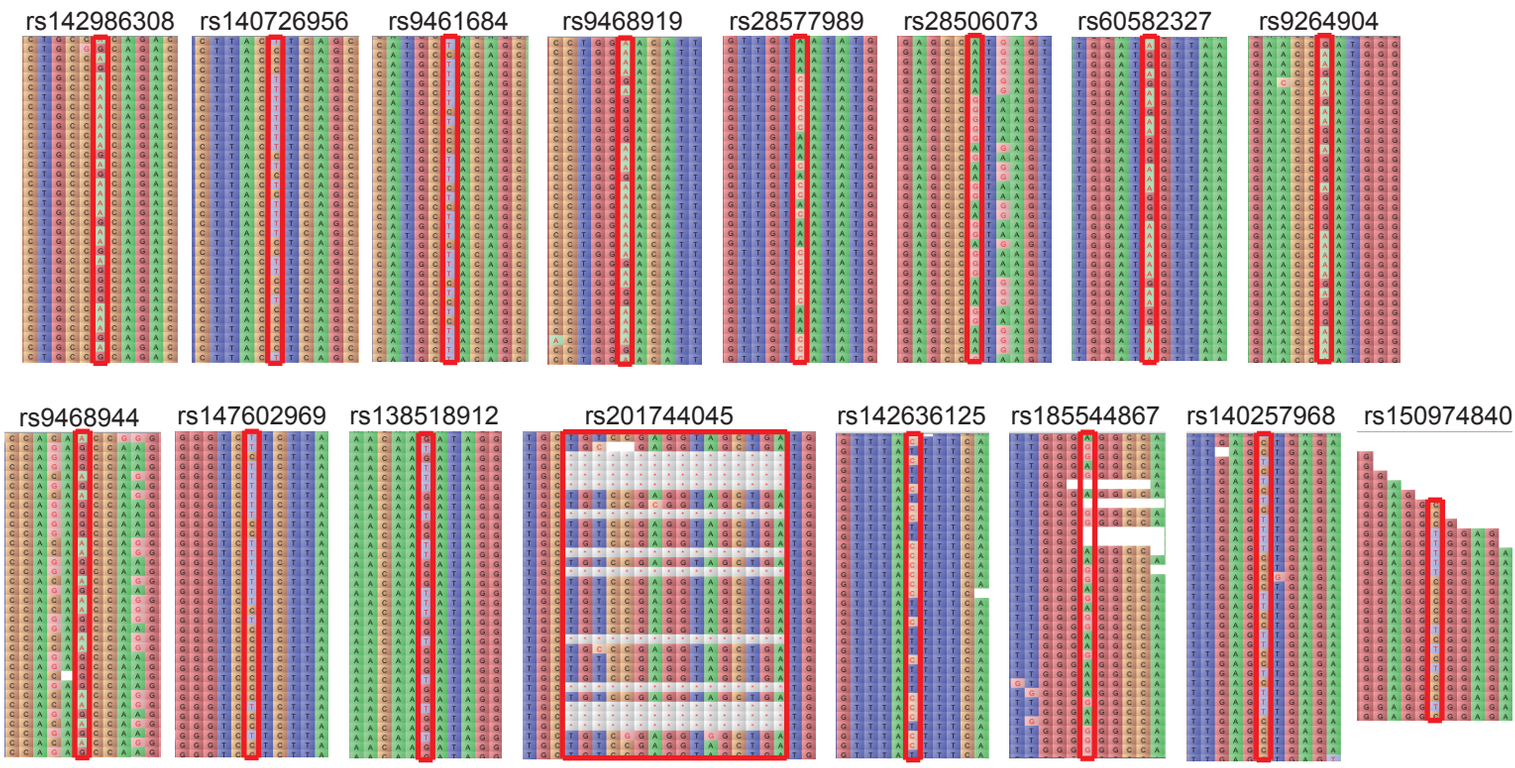

Supplementary Fig. 2. Evaluation of 16 variants extracted from all variants detected using NGS. Red squares indicate variant locations. Depicted is a portion of all sequence reads in each location derived from a single individual.

Case

Control

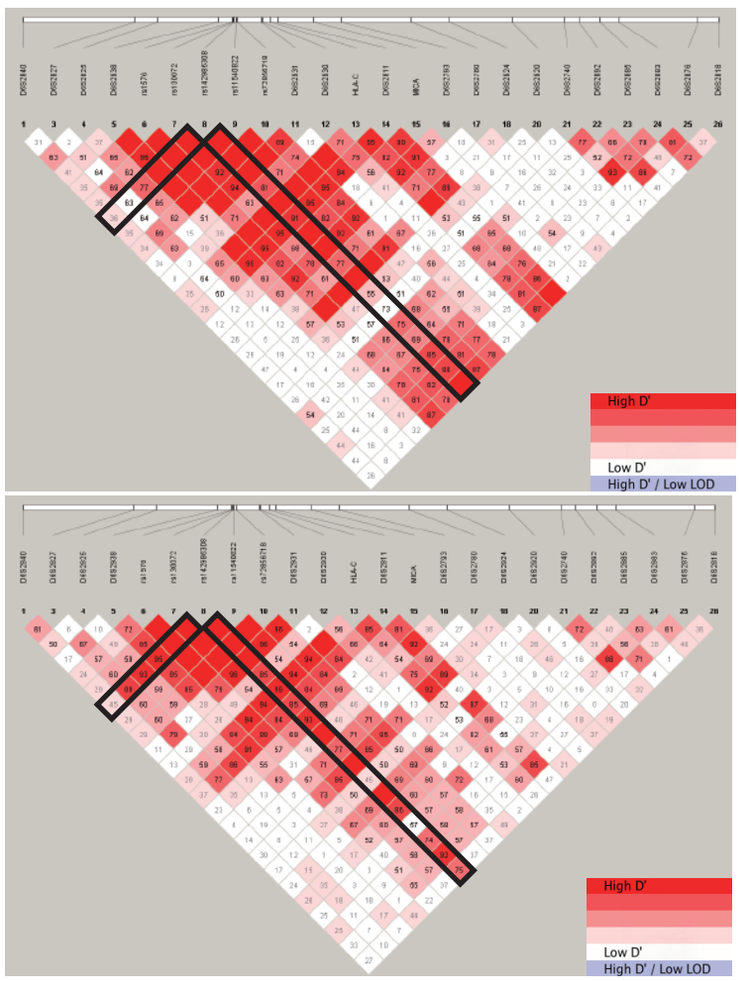

Supplementary Fig. 3. Analysis of pair-wise LD between 24 loci for investigating LD with rs142986308 in the MHC region. LD was evaluated using D' values. Black square shows locus pairs with rs142986308.

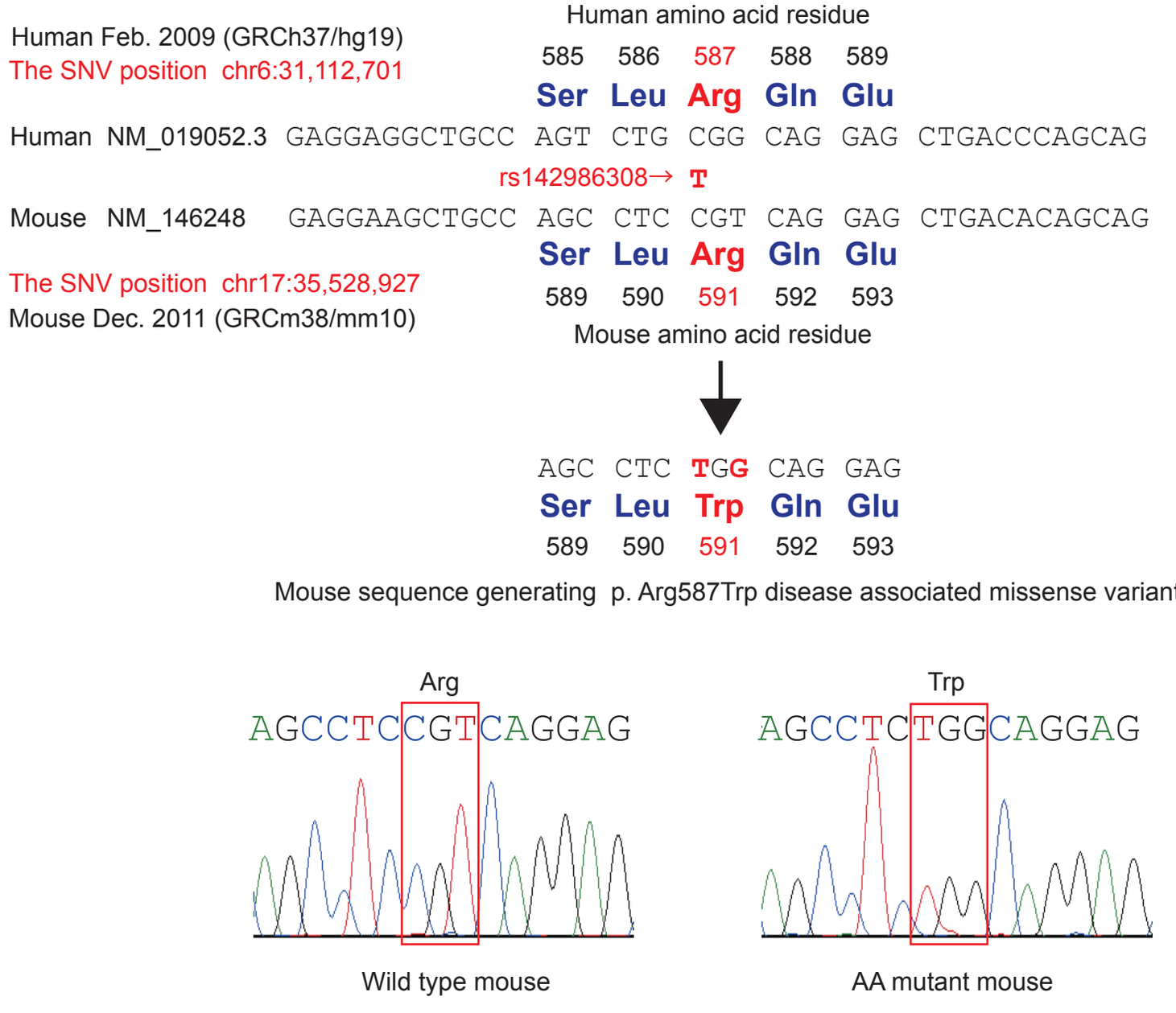

Supplementary Fig. 4. Sequence alignments of human and mouse around AA-susceptibility variant.

		Case																					
	Distance (kb)		305.9		202.4		4.9		22.6		91.6		127.4		139.6		49.9		61.4		67.2		36.4	
		67.5		78.1		142.5		27.5		121.0		237.4		69.6		174.1		72.3		266.7		80.2		
	P-value	*D6S2840*	*D6S2799*	*D6S2827*	*D6S2825*	*D6S2938*	*D6S2931*	*D6S2930*	*HLA-C*	*D6S2811*	*MICA*	*D6S2793*	*D6S2780*	*D6S2924*	*D6S2973*	*D6S2920*	*D6S2740*	*D6S2892*	*D6S2885*	*D6S2883*	*D6S2876*	*D6S2818*	*D6S2820*	*D6S2822*
Control	*D6S2840*	1.02E-01	0.03354	0.460045	0.000000	0.000000	0.014948	0.000000	0.000000	0.137533	0.000000	0.033215	0.028172	0.356390	0.235190	0.011613	0.522195	0.089233	0.188087	0.037652	0.040050	0.377232	0.660680	0.000000
	D6S2799	0.000000	1.52E-01	0.000000	0.000000	0.000000	0.166855	0.000000	0.000000	0.000530	0.121127	0.292180	0.004352	0.000795	0.636092	0.017823	0.001393	0.007137	0.000000	0.232030	0.010960	0.000623	0.266225	0.790343
	D6S2827	0.000435	0.000000	2.03E-03	0.000000	0.015330	0.000000	0.000000	0.000000	0.065188	0.012405	0.480185	0.000000	0.043575	0.000000	0.001343	0.003247	0.033243	0.000055	0.023703	0.003030	0.028065	0.368067	0.802955
	D6S2825	0.000700	0.000000	0.000000	1.66E-02	0.000000	0.009115	0.000000	0.019027	0.000000	0.000000	0.000130	0.016480	0.007620	0.749313	0.058053	0.000000	0.024823	0.000532	0.020393	0.000000	0.035795	0.438202	0.41089
	D6S2938	0.000000	0.000000	0.000000	0.000000	9.41E-03	0.000000	0.000000	0.000000	0.000000	0.000000	0.000000	0.000000	0.000000	0.107620	0.023807	0.000000	0.000000	0.000000	0.000000	0.002260	0.000000	0.008017	0.608572
	D6S2931	0.000000	0.000000	0.000000	0.000000	0.000000	9.89E-03	0.000000	0.000000	0.000000	0.000000	0.029100	0.009973	0.000858	0.000000	0.004177	0.016738	0.008710	0.000000	0.172283	0.000000	0.485823	0.136472	0.925378
	D6S2930	0.011645	0.000000	0.000000	0.000000	0.000000	0.000000	2.54E-04	0.000000	0.000000	0.000000	0.001065	0.000000	0.000000	0.205690	0.011985	0.000000	0.000000	0.000000	0.006047	0.000000	0.006152	0.211785	0.009695
	HLA-C	0.000520	0.000000	0.000000	0.000000	0.000000	0.000000	0.000000	5.33E-04	0.008285	0.000000	0.000693	0.000000	0.006122	0.006155	0.000000	0.004485	0.006298	0.000315	0.000000	0.053353	0.005483	0.336927	0.371948
	D6S2811	0.003787	0.000000	0.000000	0.000000	0.000000	0.012497	0.000000	0.014882	3.39E-05	0.000000	0.000000	0.000000	0.008750	0.217195	0.010305	0.033510	0.014485	0.006030	0.005530	0.000000	0.005450	0.084005	0.248908
	MICA	0.000000	0.000000	0.000000	0.000000	0.000000	0.000000	0.000000	0.000000	0.000000	6.77E-03	0.000000	0.000505	0.015975	0.240617	0.000000	0.000640	0.000000	0.000000	0.000000	0.017643	0.051910	0.080340	0.250442
	D6S2793	0.000467	0.000000	0.000000	0.000000	0.000000	0.000000	0.000000	0.000000	0.000000	0.000000	8.92E-03	0.000000	0.046578	0.107305	0.000000	0.004300	0.000000	0.000000	0.000000	0.000150	0.008385	0.023318	0.044807
	D6S2780	0.000000	0.000000	0.002978	0.000000	0.000000	0.000000	0.000000	0.000000	0.000000	0.000000	0.000000	5.43E-02	0.000000	0.281443	0.000000	0.000530	0.000000	0.000000	0.000000	0.069150	0.000000	0.005403	0.673458
	D6S2924	0.000000	0.000000	0.000000	0.000000	0.000000	0.000000	0.000000	0.000000	0.000000	0.000000	0.000000	0.000000	1.10E-01	0.000003	0.000000	0.000000	0.161863	0.004367	0.951215	0.683435	0.537070	0.851222	0.166038
	D6S2973	0.173595	0.050872	0.000000	0.039782	0.008392	0.003482	0.000000	0.000000	0.002357	0.000442	0.000993	0.000000	0.000000	1.00E-01	0.000000	0.044888	0.044153	0.033405	0.052192	0.000070	0.008617	0.619723	0.51522
	D6S2920	0.002785	0.000000	0.000000	0.000000	0.000000	0.000000	0.000000	0.001870	0.000000	0.000000	0.000000	0.000000	0.000000	0.000000	3.80E-02	0.000000	0.000000	0.000000	0.000000	0.000000	0.052860	0.344975	0.069652
	D6S2740	0.000000	0.000000	0.000000	0.000000	0.000000	0.000000	0.000000	0.000000	0.000000	0.000000	0.000000	0.000000	0.000000	0.266825	0.000000	1.16E-03	0.000000	0.000000	0.000000	0.000000	0.157630	0.810777	0.084828
	D6S2892	0.004180	0.000000	0.000000	0.000000	0.000000	0.005375	0.000000	0.000000	0.005667	0.000000	0.000000	0.000000	0.000000	0.004067	0.000000	0.000000	2.02E-01	0.000000	0.000000	0.000000	0.000000	0.009912	0.021235
	D6S2885	0.027145	0.000000	0.000000	0.000000	0.000000	0.007312	0.000000	0.000000	0.000000	0.000000	0.000000	0.001180	0.000000	0.000000	0.000000	0.000000	0.000000	1.34E-02	0.000000	0.000000	0.003940	0.011452	0.078000
	D6S2883	0.000000	0.000000	0.000000	0.000000	0.000000	0.000000	0.000000	0.000000	0.000000	0.000000	0.000000	0.000000	0.000000	0.000027	0.000000	0.000000	0.000000	0.000000	1.71E-02	0.000000	0.000000	0.425097	0.251512
	D6S2876	0.000000	0.000000	0.000000	0.000000	0.000000	0.000000	0.000000	0.000000	0.000000	0.000000	0.000000	0.000000	0.000000	0.000000	0.000000	0.000000	0.000000	0.000000	0.000000	1.42E-01	0.000000	0.028315	0.112567
	D6S2818	0.000000	0.000000	0.000035	0.000000	0.000000	0.000000	0.000000	0.000000	0.000000	0.000000	0.000000	0.000000	0.000000	0.000035	0.000000	0.000000	0.000000	0.000000	0.000000	0.000000	2.63E-03	0.006992	0.000803
	D6S2820	0.909760	0.505600	0.274785	0.602112	0.005085	0.780338	0.571630	0.083208	0.001618	0.682800	0.001568	0.043568	0.005665	0.816960	0.145178	0.271165	0.549437	0.099305	0.000000	0.000000	0.000210	9.39E-01	0.481575
	D6S2822	0.023187	0.002832	0.031367	0.000000	0.042445	0.003987	0.000000	0.000000	0.044338	0.052980	0.119748	0.000000	0.005840	0.000000	0.000220	0.004143	0.043088	0.000000	0.000000	0.000000	0.003737	0.000673	1.40E-01

Supplementary Fig. 5. Evaluation of pair-wise linkage disequilibrium (LD) between 23 multi-allelic loci in the MHC region.

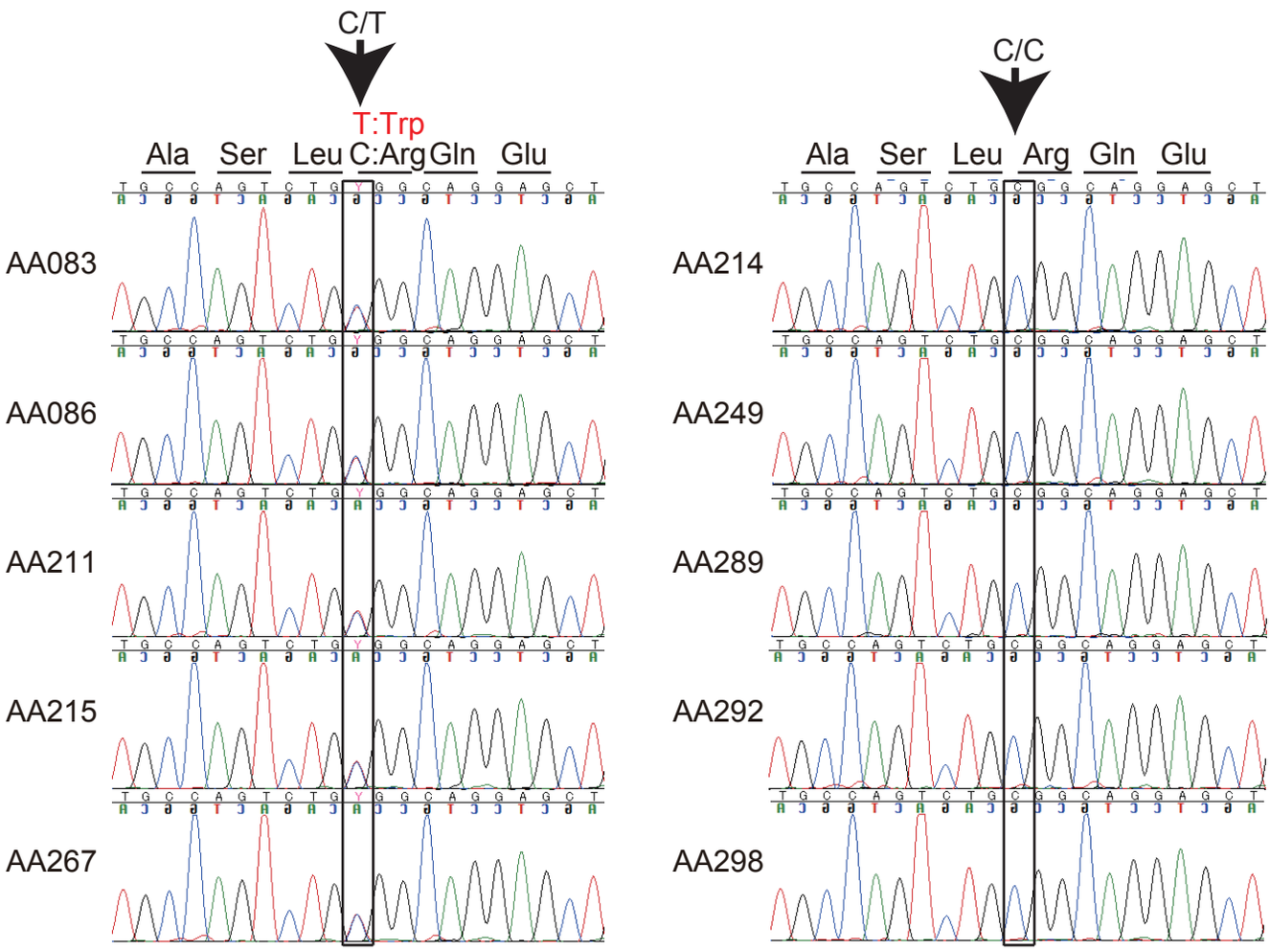

Supplementary Fig. 6. Sanger sequencing confirmation of rs142986308.

Left panel indicates individuals with heterozygous (C/T) variant. Right panel indicates individuals with homozygous (C/C) variant. Black squares and arrows indicate position of rs142986308. Codons in the *CCHCR1* gene are shown in the upper layer.

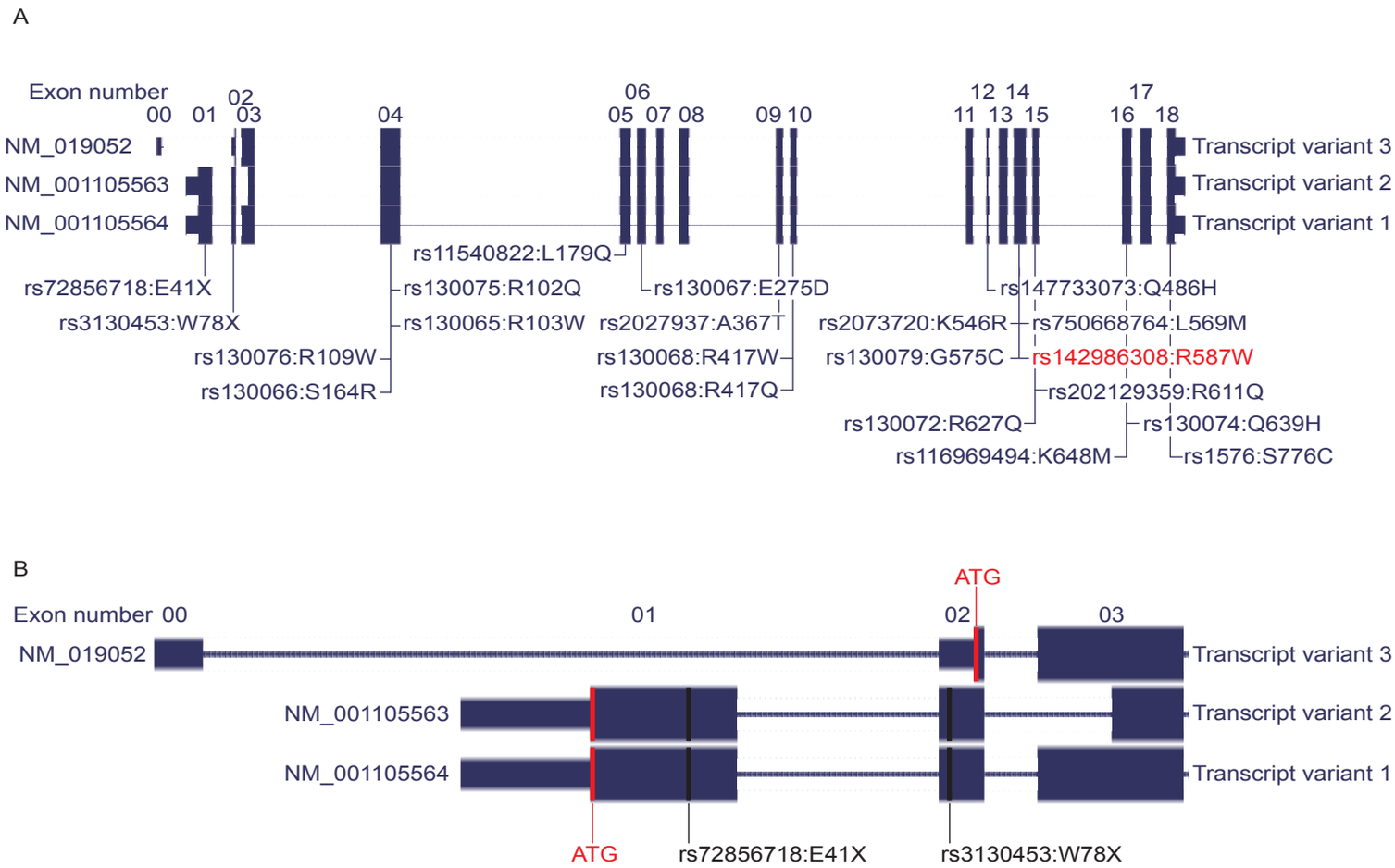

Supplementary Fig. 7. Schematic overview of *CCHCR1* gene structure and variants with amino acid substitution.

Three alternative splicing variants in *CCHCR1* are in the RefSeq Genes database. (A) Twenty-two variants lie in this gene. Red indicates the variant (rs142986308) identified by resequencing in the MHC region. (B) The difference for each transcript variant exists in the 5' region of *CCHCR1*. Two ATG initiation codons and 2 common nonsense variants were observed in exon01 and exon02.

These two nonsense variants were mapped to the coding regions in alternative transcripts 1 and 2, which are common in Japanese and European Americans, and to the non-coding region in alternative transcript 3. SNV rs3130453 gave rise to the shortest of the 3 alternative transcripts previously reported for *CCHCR1* (PLoS One 7(11):e49920) and SNV rs72856718, which had not been reported and was predicted to result in the same alternative transcript.

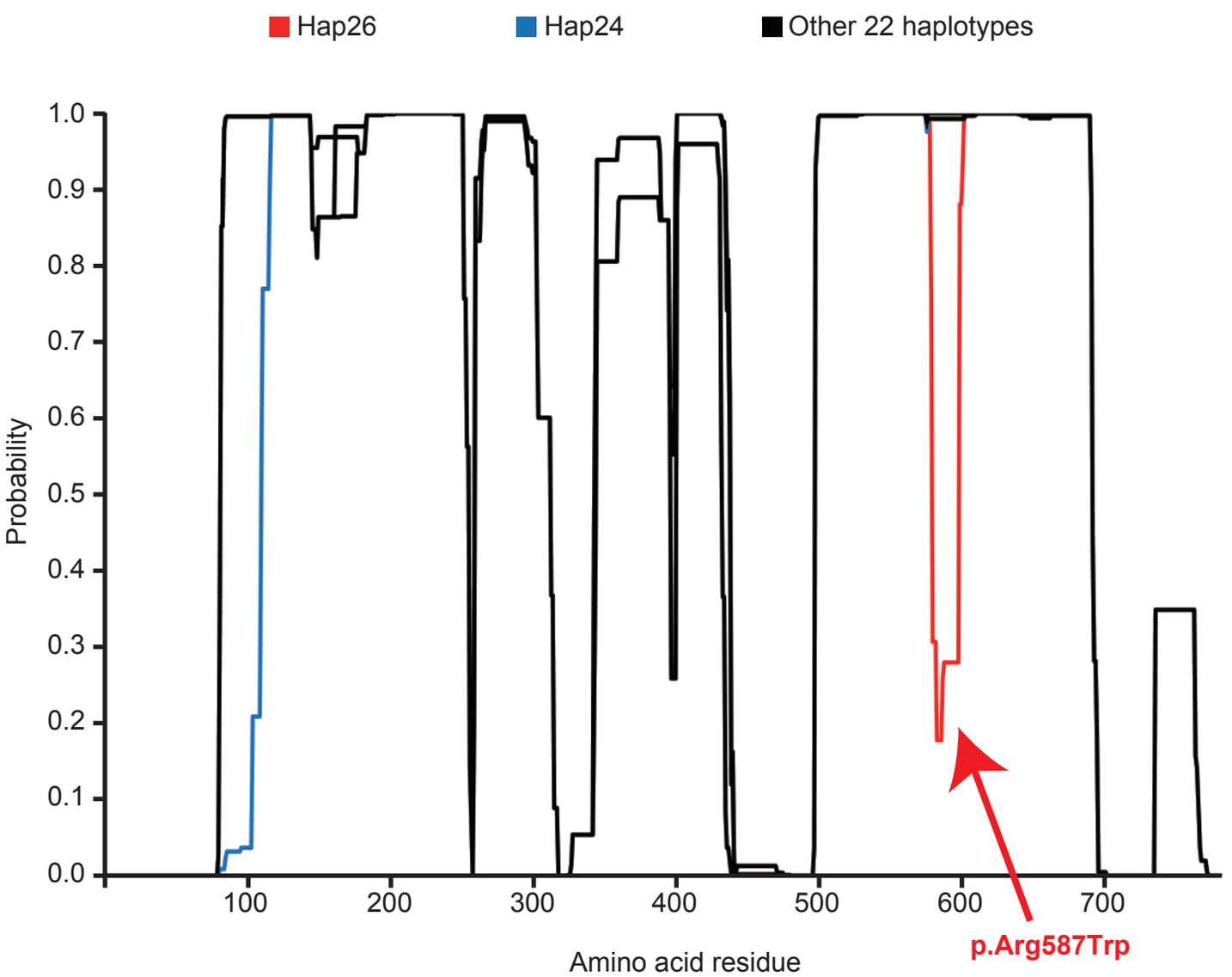

Supplementary Fig. 8. Coiled-coil structure prediction of CCHCR1 in 26 haplotypes using COILS, v. 2.2

Y axis indicated the probability of coiled-coil conformation. X axis indicates amino acid residue number. Arrow shows position of p.Arg587Trp (rs142986308).

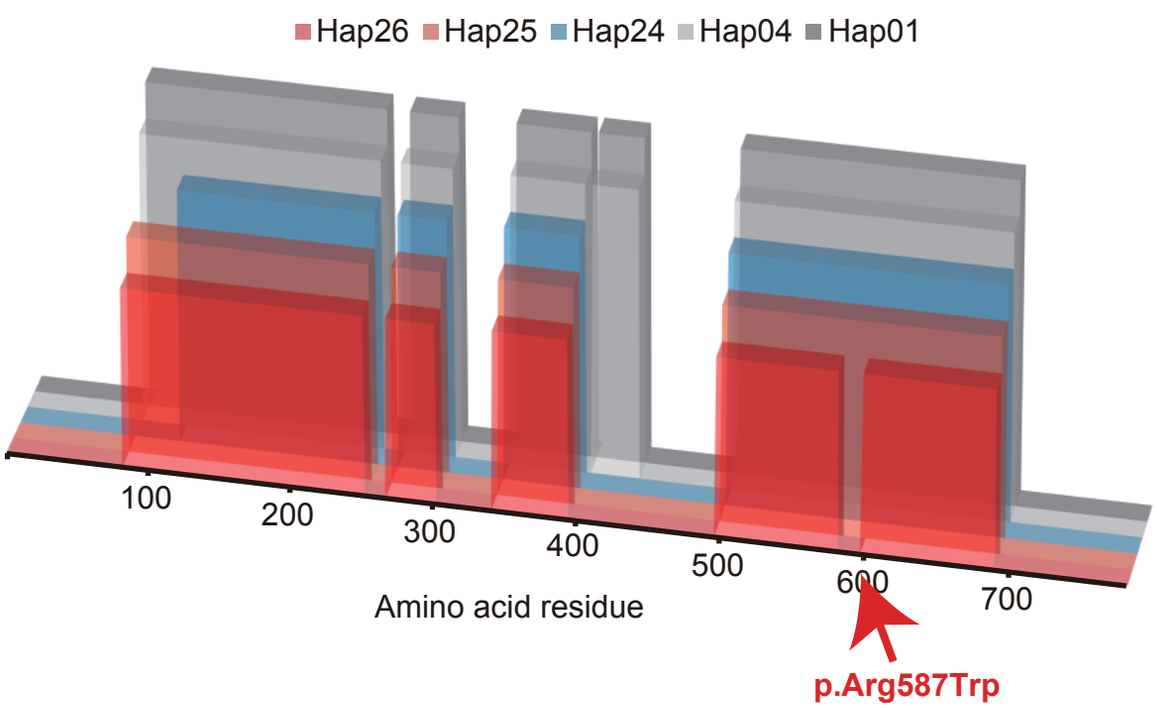

Supplementary Fig. 9. Coiled-coil structure prediction of CCHCR1 in 5 selected haplotypes using Paircoil2. X axis indicates amino acid residue number. *P*-value cutoff of 0.025 was used as the default setting for domain prediction. Colored boxes indicate segments predicted to form coiled-coil domains. Arrow shows position of p.Arg587Trp (rs142986308).

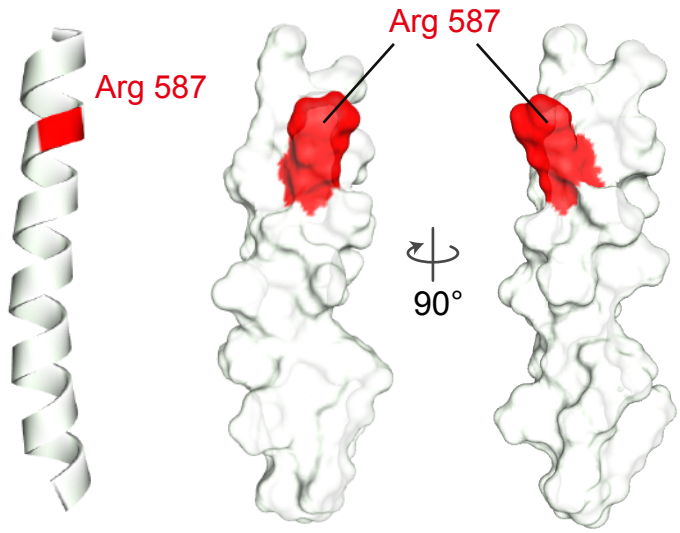

Supplementary Fig.10. Ribbon and molecular surface representations of partial CCHCR1 structure. Surface models are shown in 2 orientations. Residue 587 is represented in red.

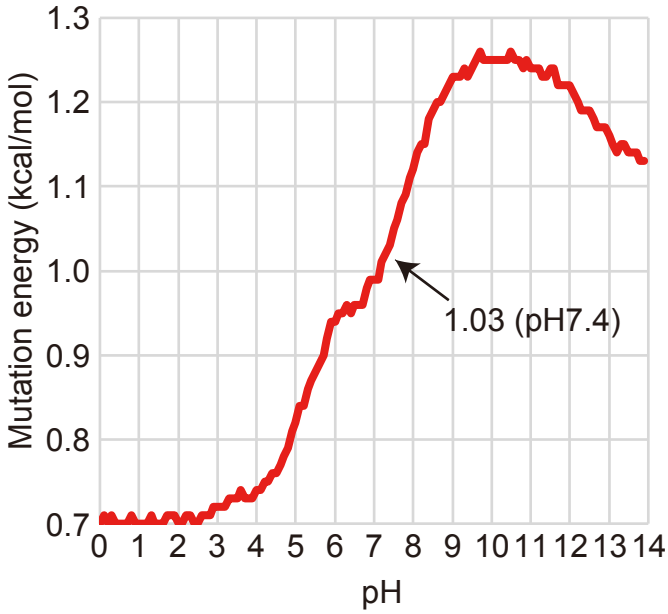

Supplementary Fig.11. Effects of Arg587Trp mutation on CCHCR1 protein structure at different pH values. A change of >0.5 cal/mol, which destabilized the structure, was classified as a significant change.

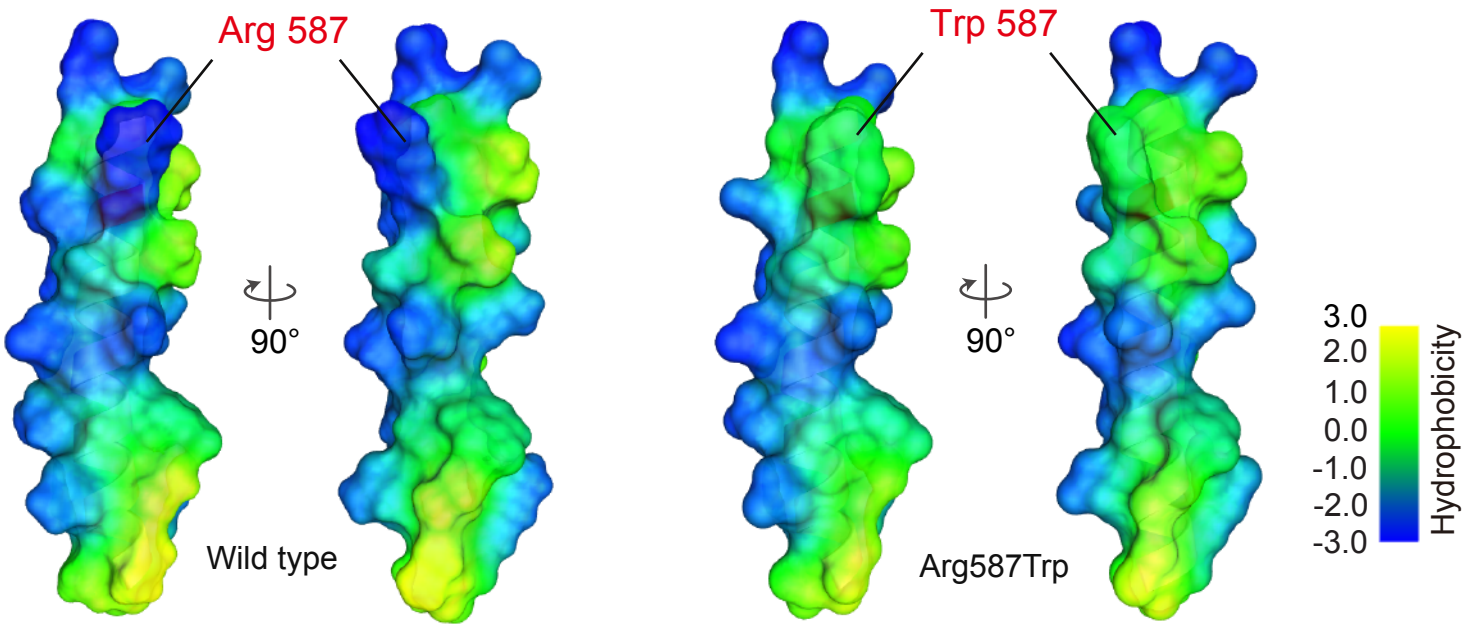

Supplementary Fig.12. Surface maps showing hydrophobicity of the wild type and Arg587Trp are presented.

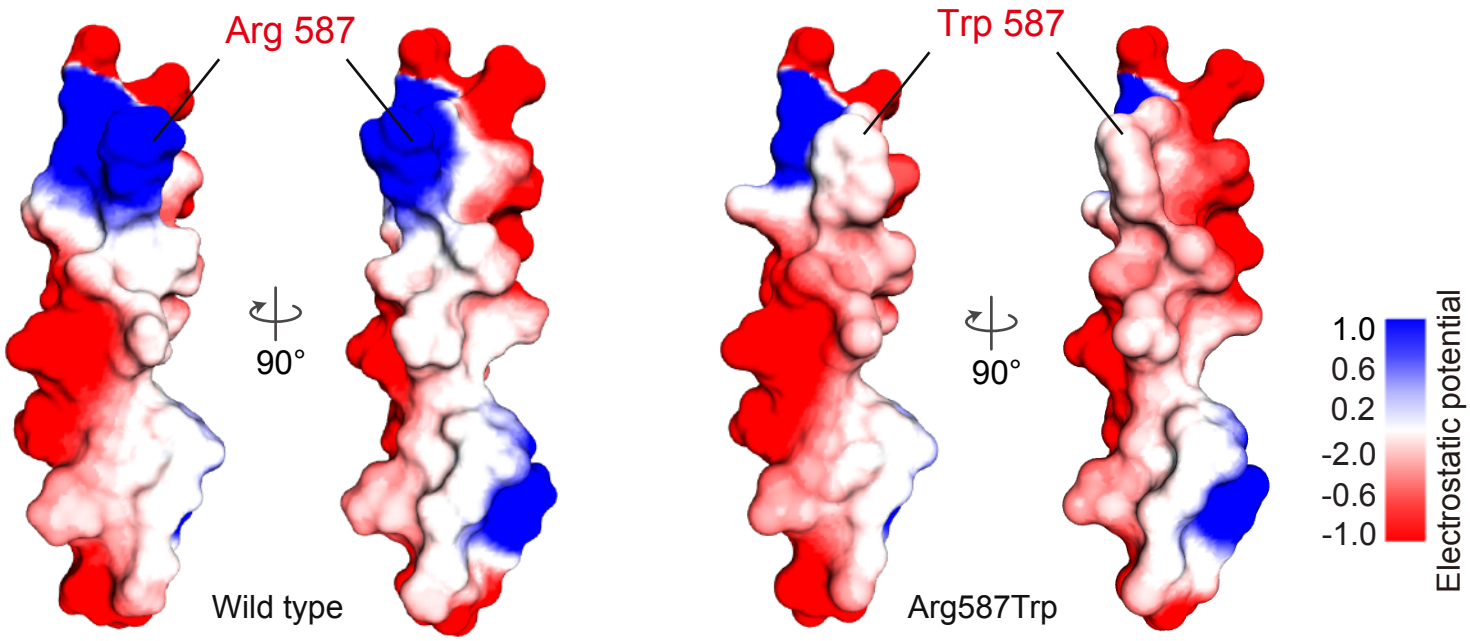

Supplementary Fig.13. Surface maps showing electrostatic potential of the wild type and Arg587Trp are presented.

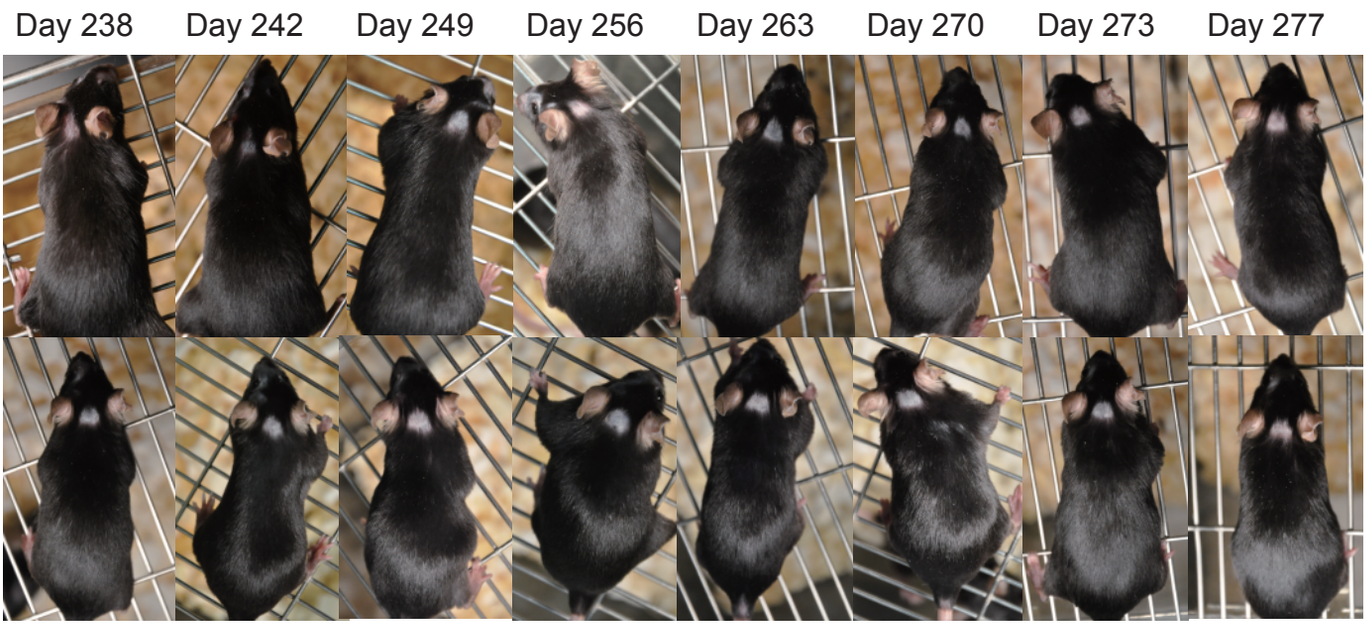

Supplementary Fig.14. Fixed hair loss area in representative Cchcr1-hom mouse after onset of hair loss.

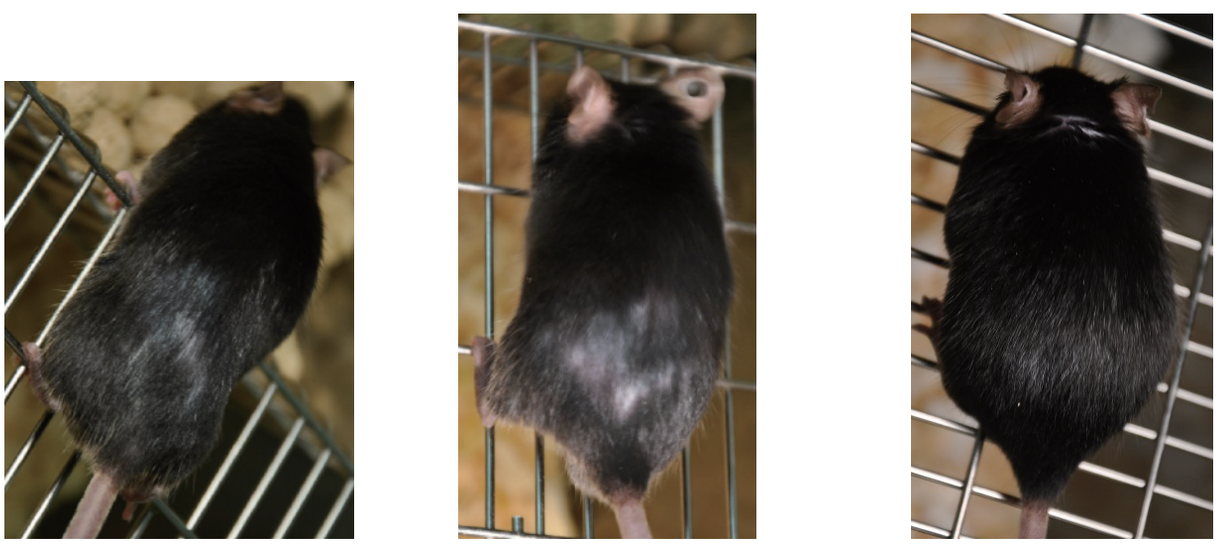

Supplementary Fig. 15. Hair loss area recovered in representative Cchcr1-hom mouse.

Supplementary Fig.16. Various type of hair loss area in Cchcr1 mice

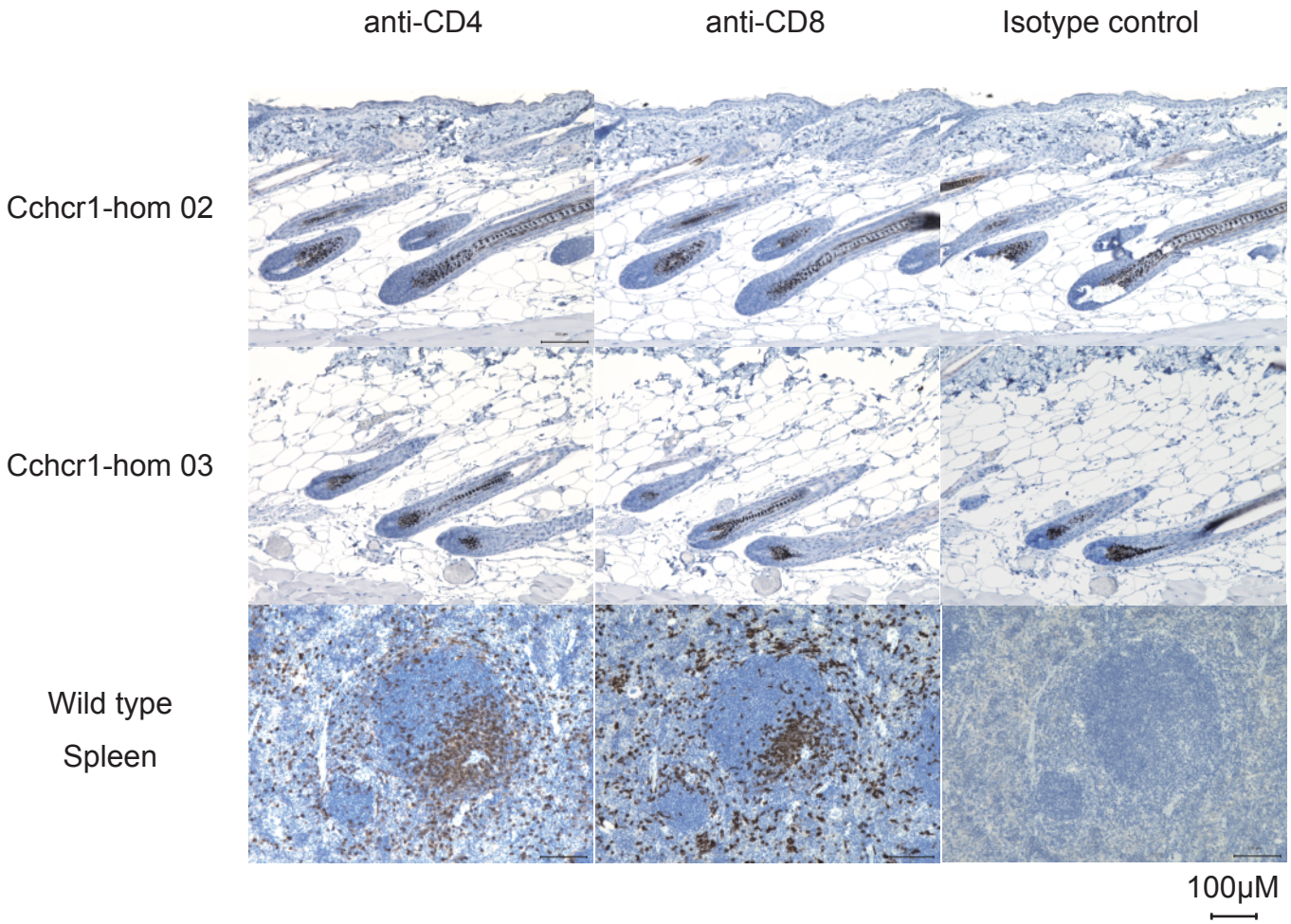

Supplementary Fig. 17. Immunostaininig of skin biopsies Cchcr1-hom mice were performed by anti-CD4 and CD8 anitbodies with hematoxylin. Spleen of a wild type mouse was used as the positive control.

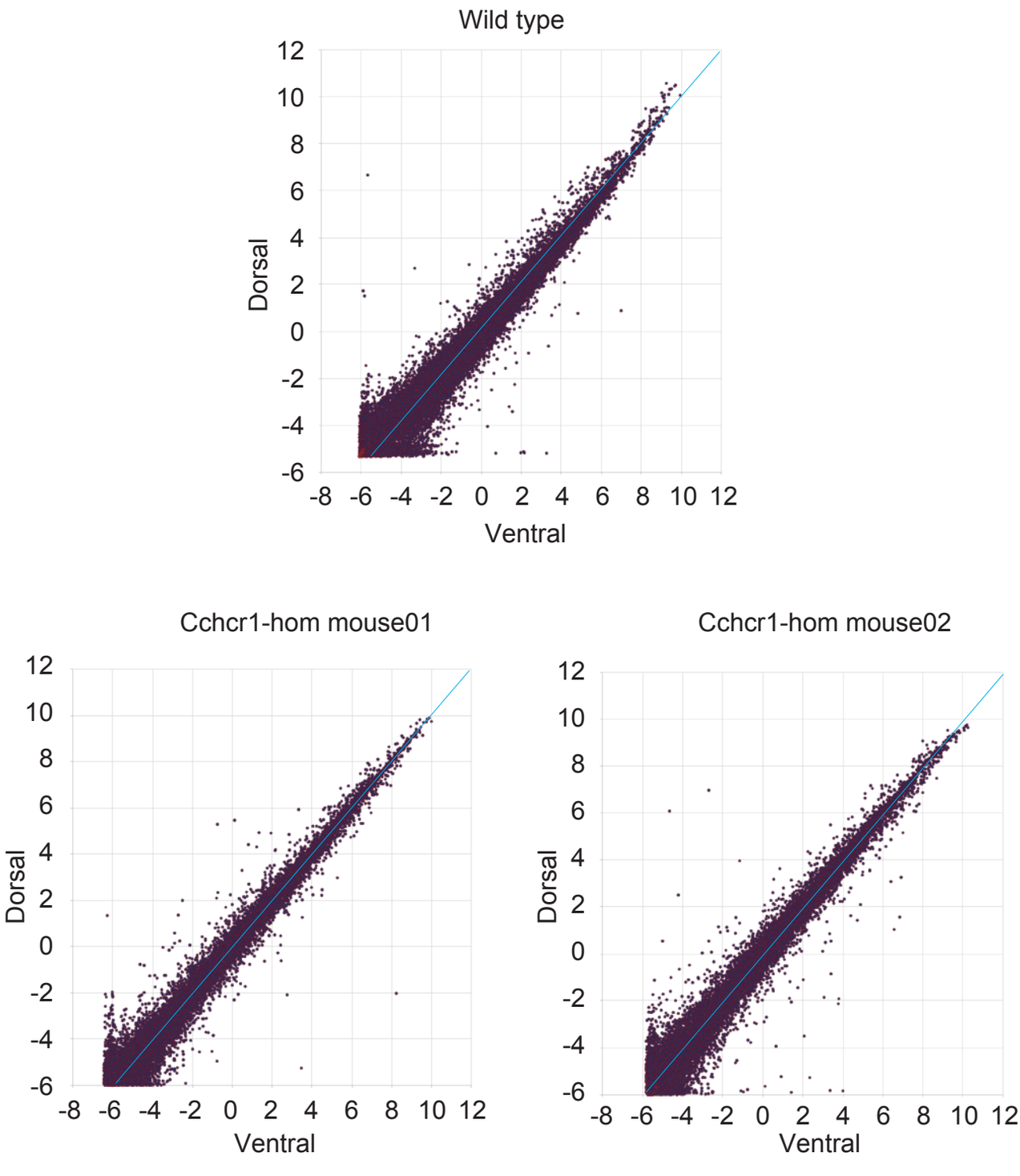

Supplementary Fig. 18. Scatter plot between dorsal and ventral skins in the same individual.

In each panel, the both axis indicate normalized expression values of 28,425 probes with gene symbol.

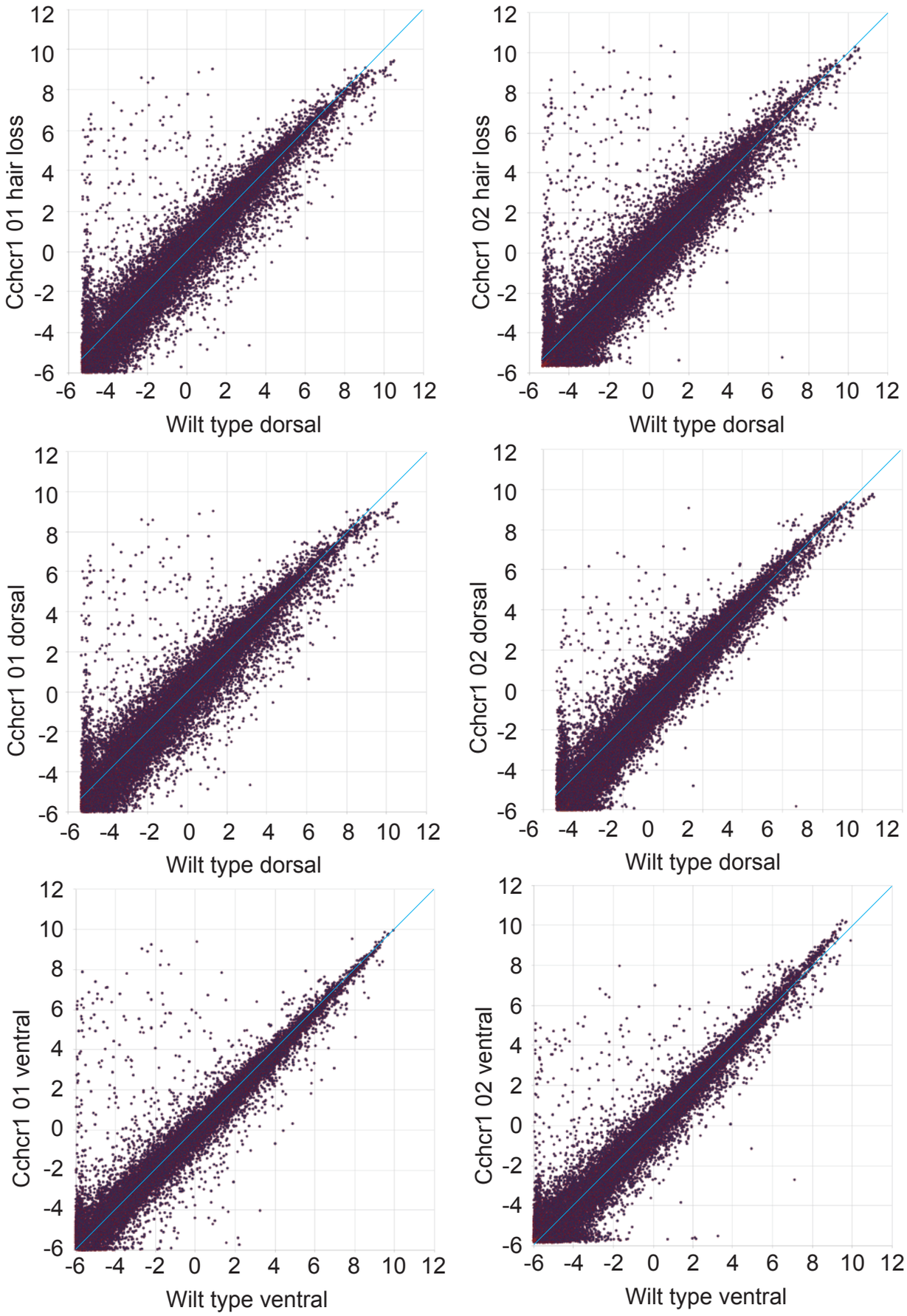

Supplementary Fig. 19. **Scatter plots between AA mouse and wild type skin.**

In each panel, the both axis indicate normalized expression values of 28,425 probes with gene symbol.

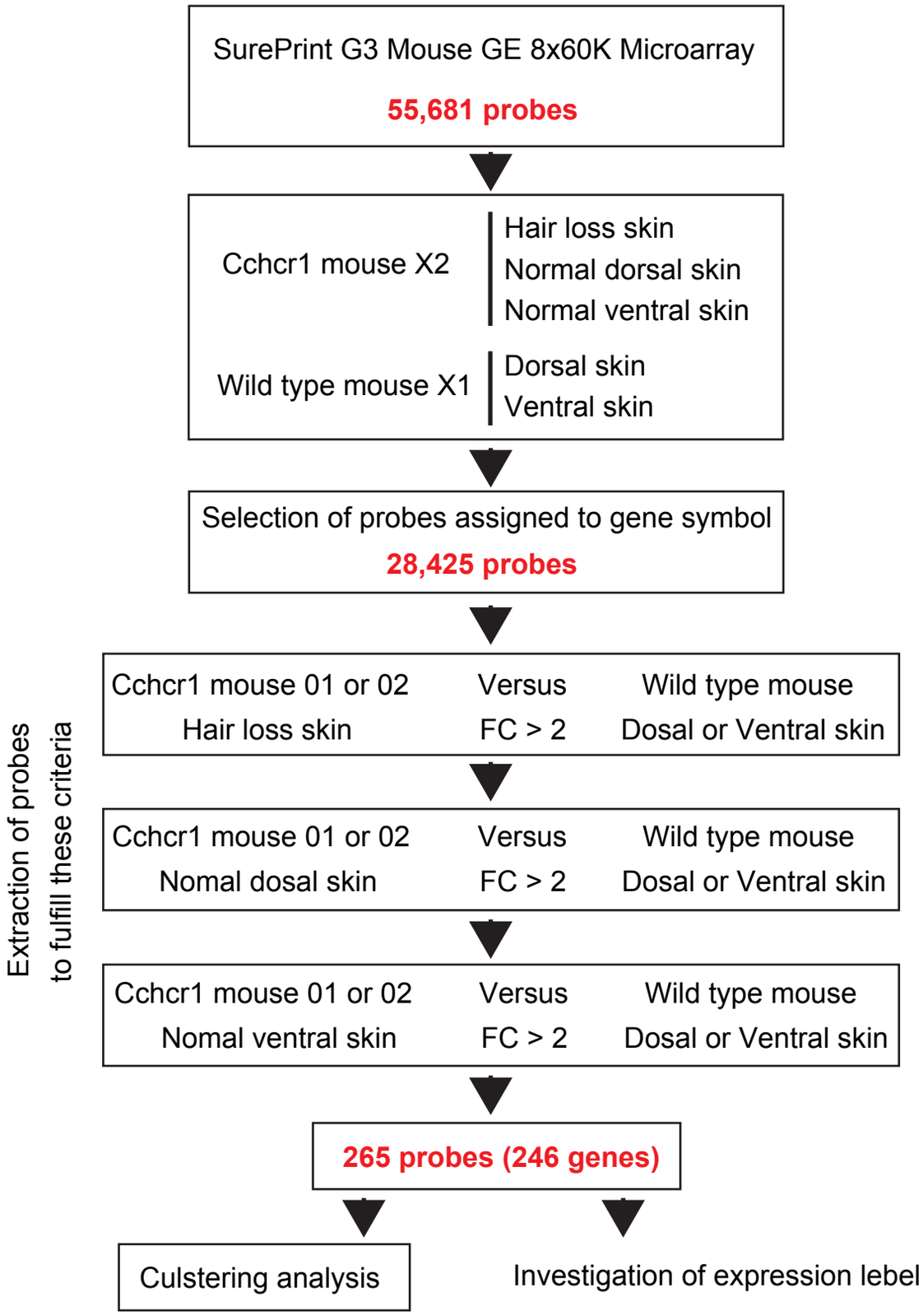

Supplementary Fig. 20. **Filtering scheme used for microarray analysis.**
Scatter plots of normalized expression values indicated no expression differentiations between each dorsal and ventral skin within the same individual (Supplementary Fig.18). On the other hand, all comparisons of Cchcr1 mice with wild type indicated mainly up-regulated probes in Cchcr1 mice (Supplementary Fig.19). Therefore, we attempted to extract probes showing 2-fold up or down regulation in all comparisons of AA mice with wild type, demonstrating 265 probes (246 genes) were obtained as candidates for next targets.

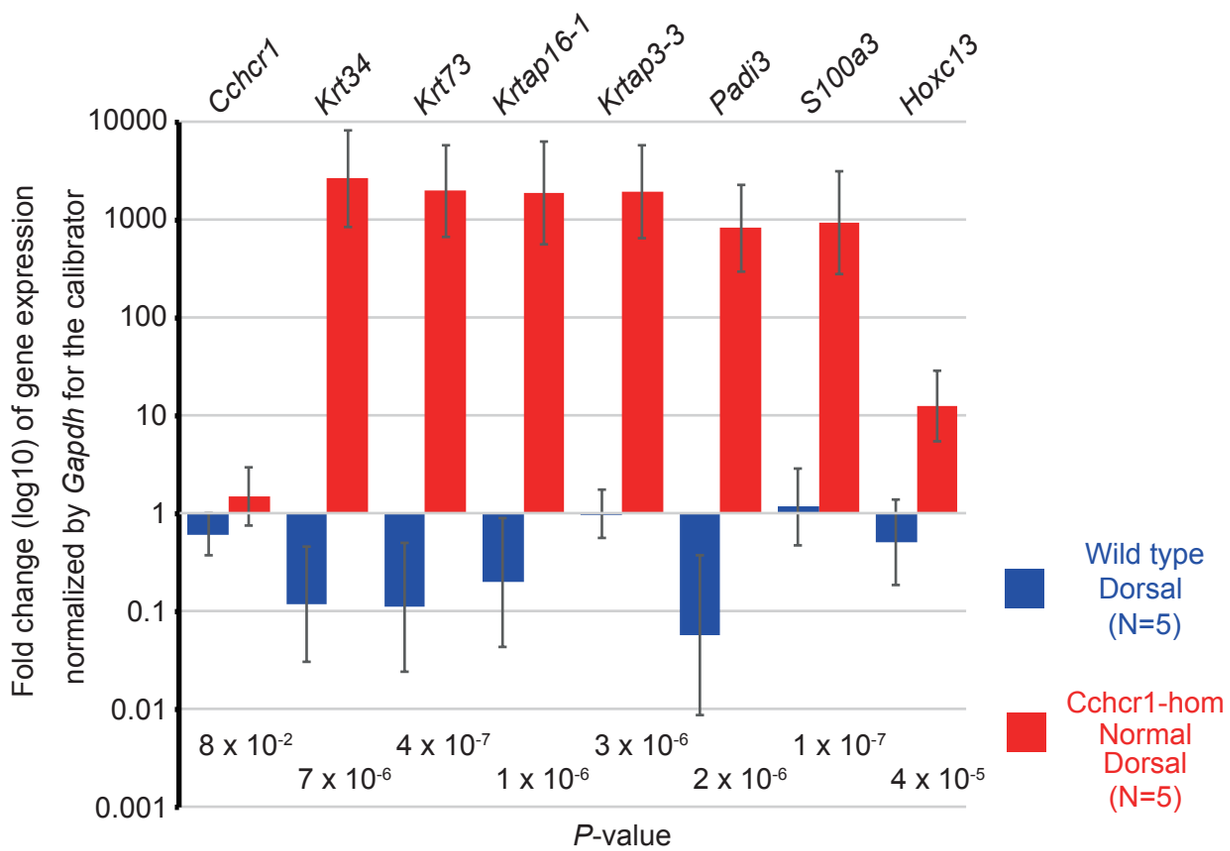

Supplementary Fig. 21. Analysis of expression in mouse skin using quantitative PCR and a comparative CT method. Each column is added to 95% confidence interval as a bar. Fold change values were calculated by applying normal dorsal skin from a wild-type mouse to the calibrator. Thus, the fold change value in the calibrator always was one. Statistical significance was determined using Welch' s t test.

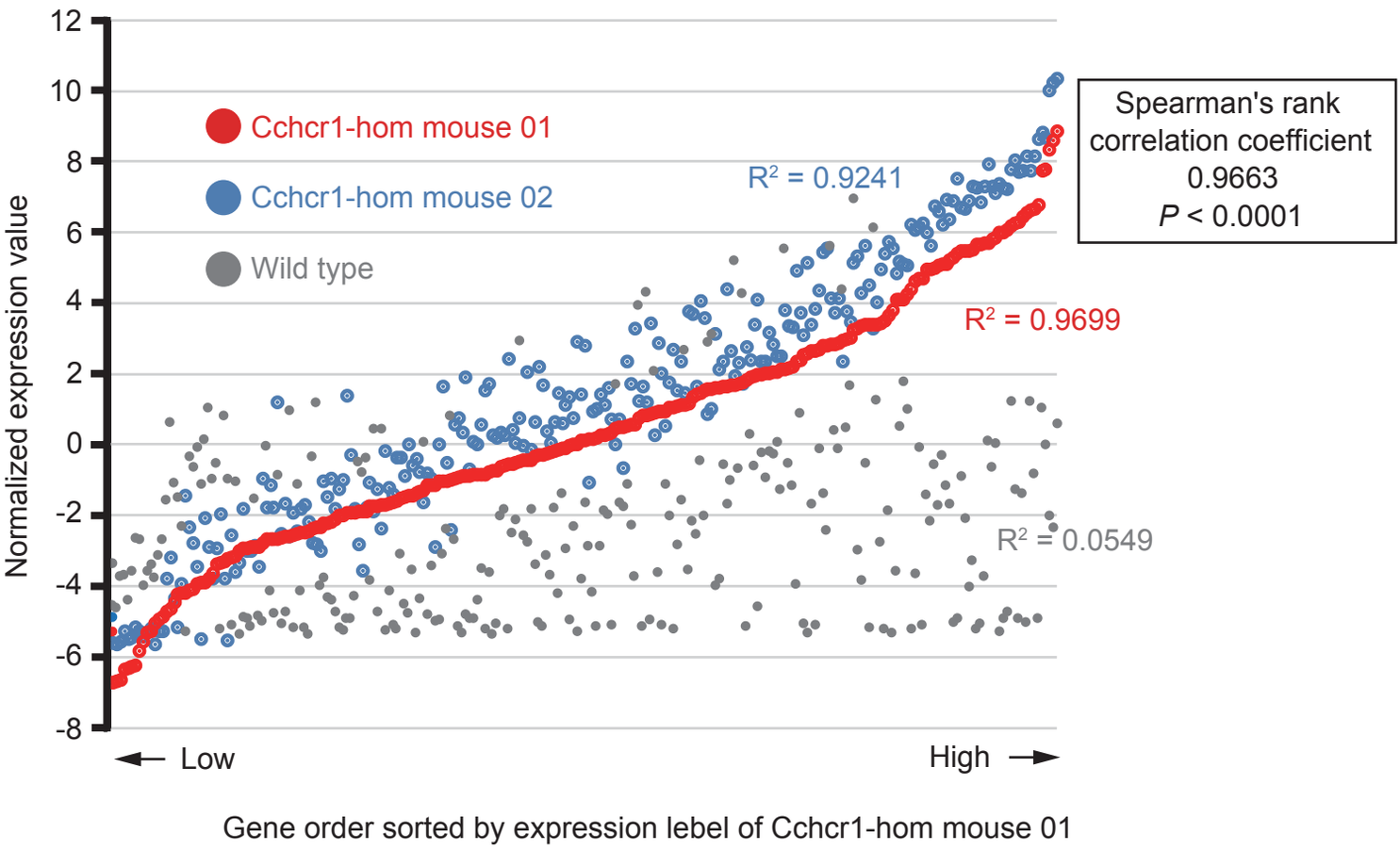

Supplementary Fig. 22. Gene expression trends in skin biopsies from Cchcr1-hom mouse 01 and 02 using 265 probes that showed a ≥2-fold change. Correlation coefficients are indicated for each mouse. Correlation coefficients and statistical significance was determined with Spearman's rho between Cchcr1-hom mouse 01 and 02.

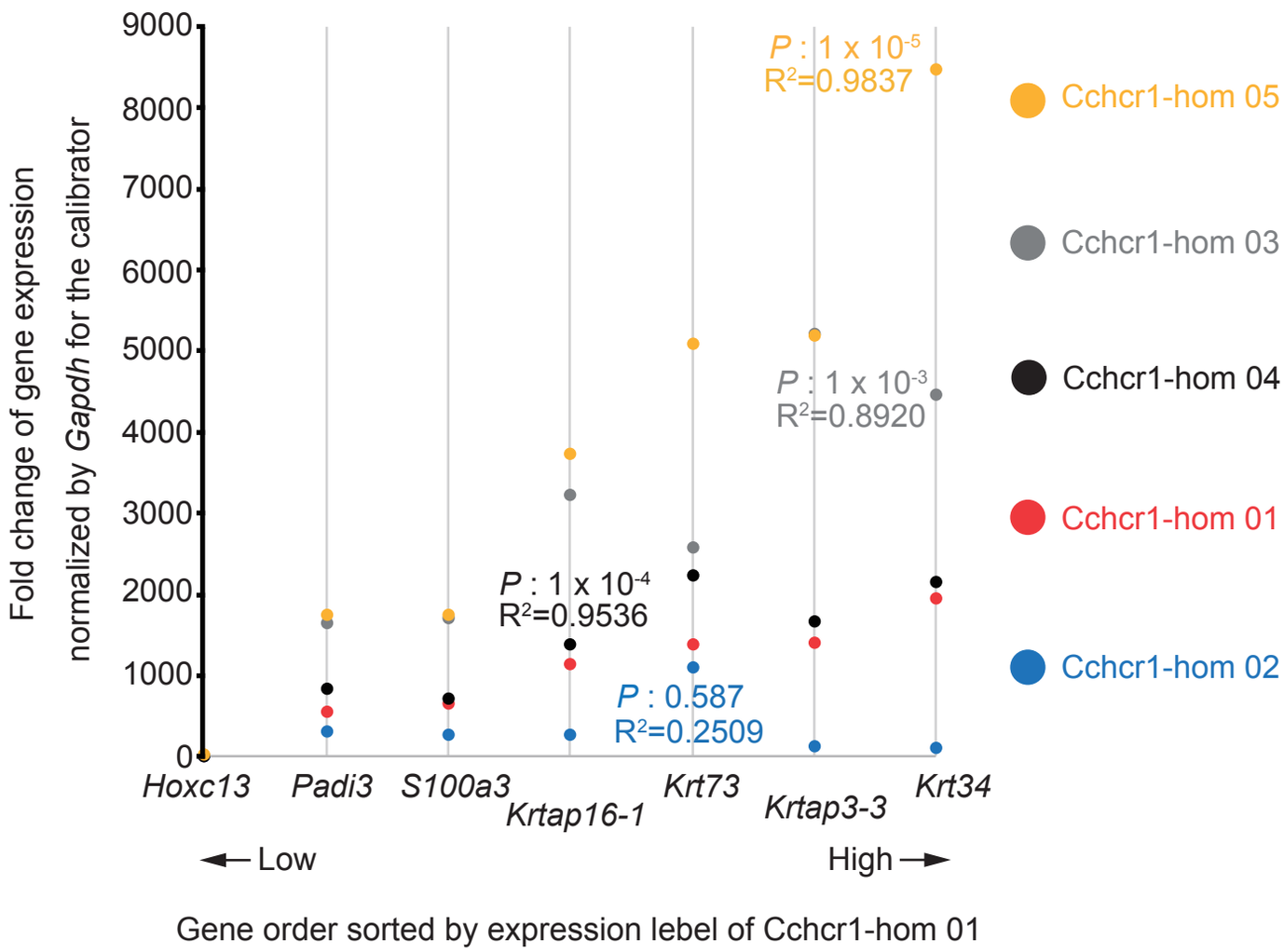

Supplementary Fig. 23. Gene expression trends in skin biopsies from dorsal normal areas in Cchcr1-hom mice. Correlation coefficients and the statistical significance was determined using Pearson's product-moment correlation between each mouse and Cchcr1-hom 01.

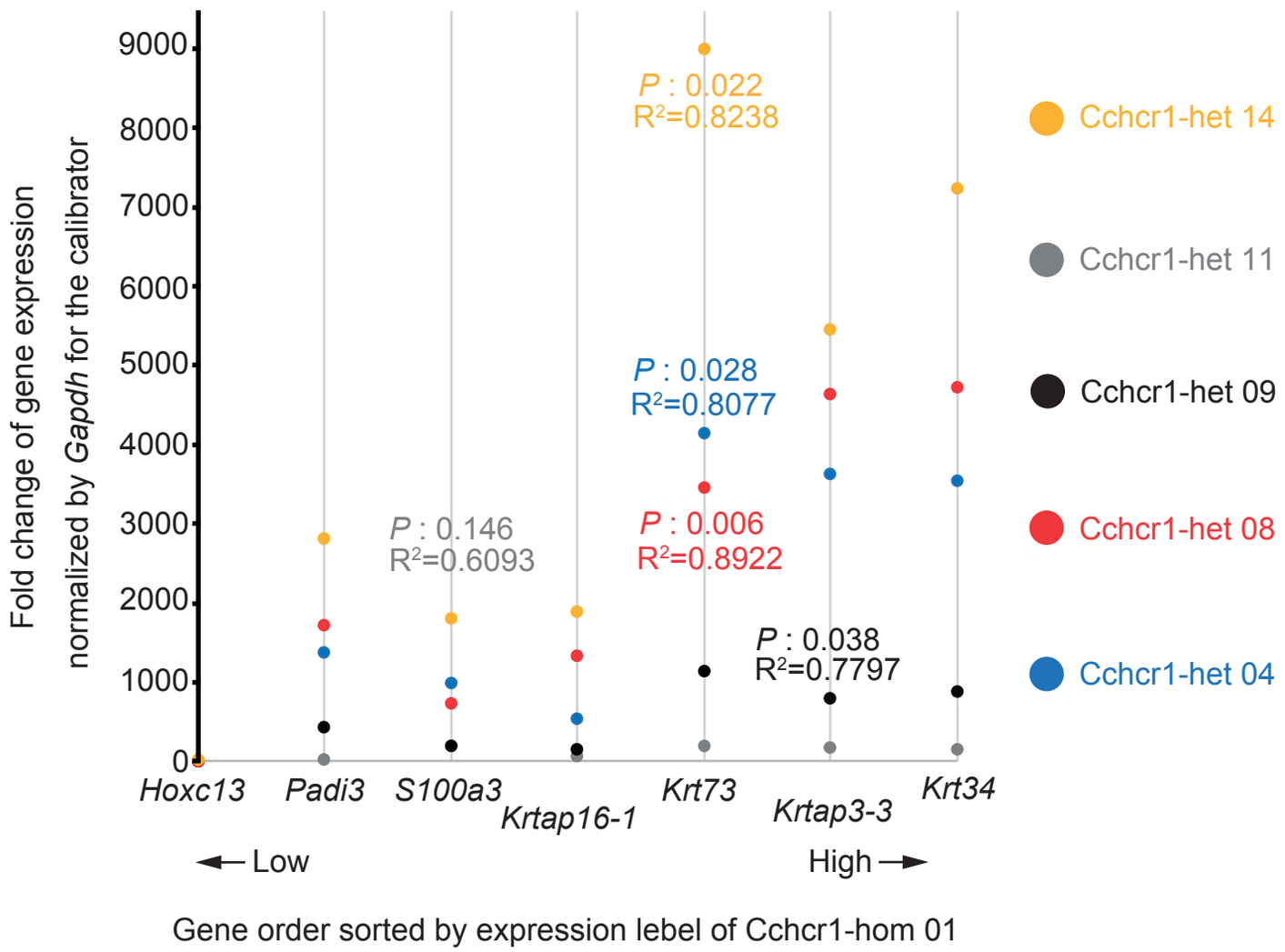

Supplementary Fig. 24. Gene expression trends in skin biopsies from dorsal normal areas in Cchcr1-het mice. Correlation coefficients and the statistical significance was determined using Pearson's product-moment correlation between each mouse and Cchcr1-hom 01.

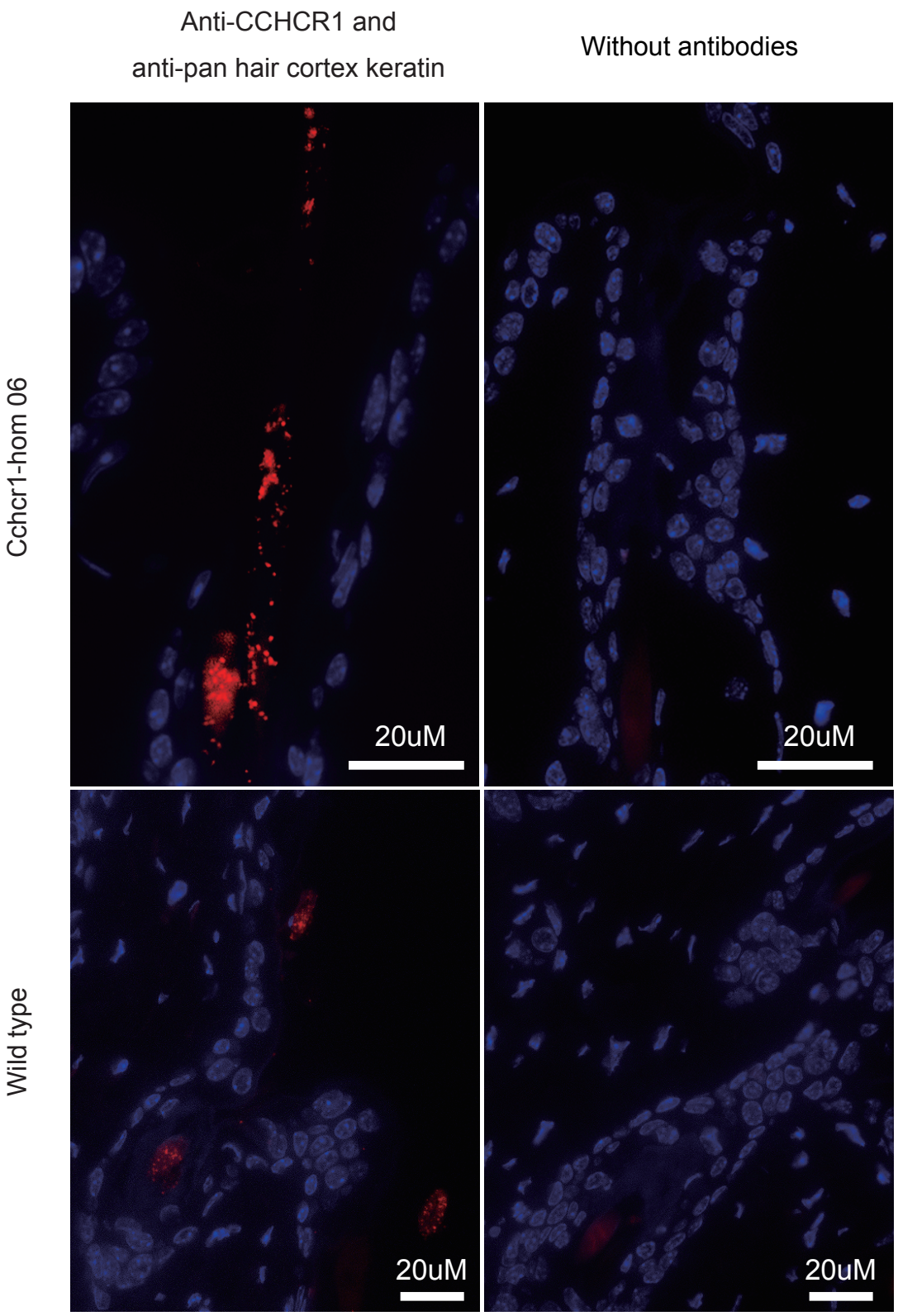

Supplementary Fig. 25. Proximity Ligation Assay (PLA) detected protein–protein interaction between CCHCR1 and hair cortex keratin in Cchcr1-hom and wild type mice.

Red dots indicate signals of the interaction in the left panels. Slight red smears indicate the background by PLA in all panels. Upper panels show longitudinal section of upper hair follicle from Cchcr1-hom mouse. Lower panels show cross sectional section of upper hair follicle from wild type mouse.

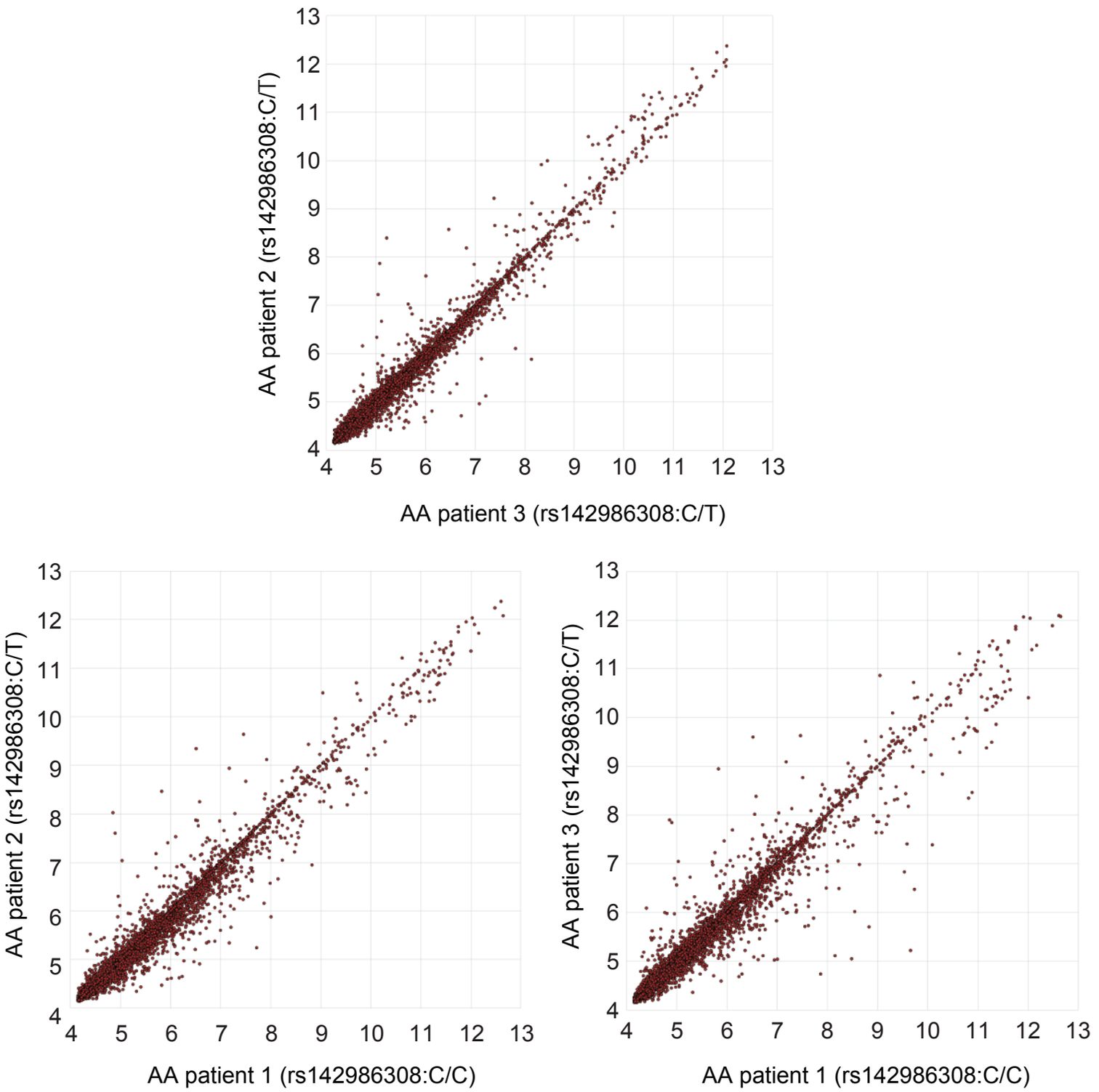

Supplementary Fig. 26. Scatter plot of normalized signal between each patient. In each panel, the both axis indicate normalized expression values of 22,887 Transcripts Cluster with gene symbol.

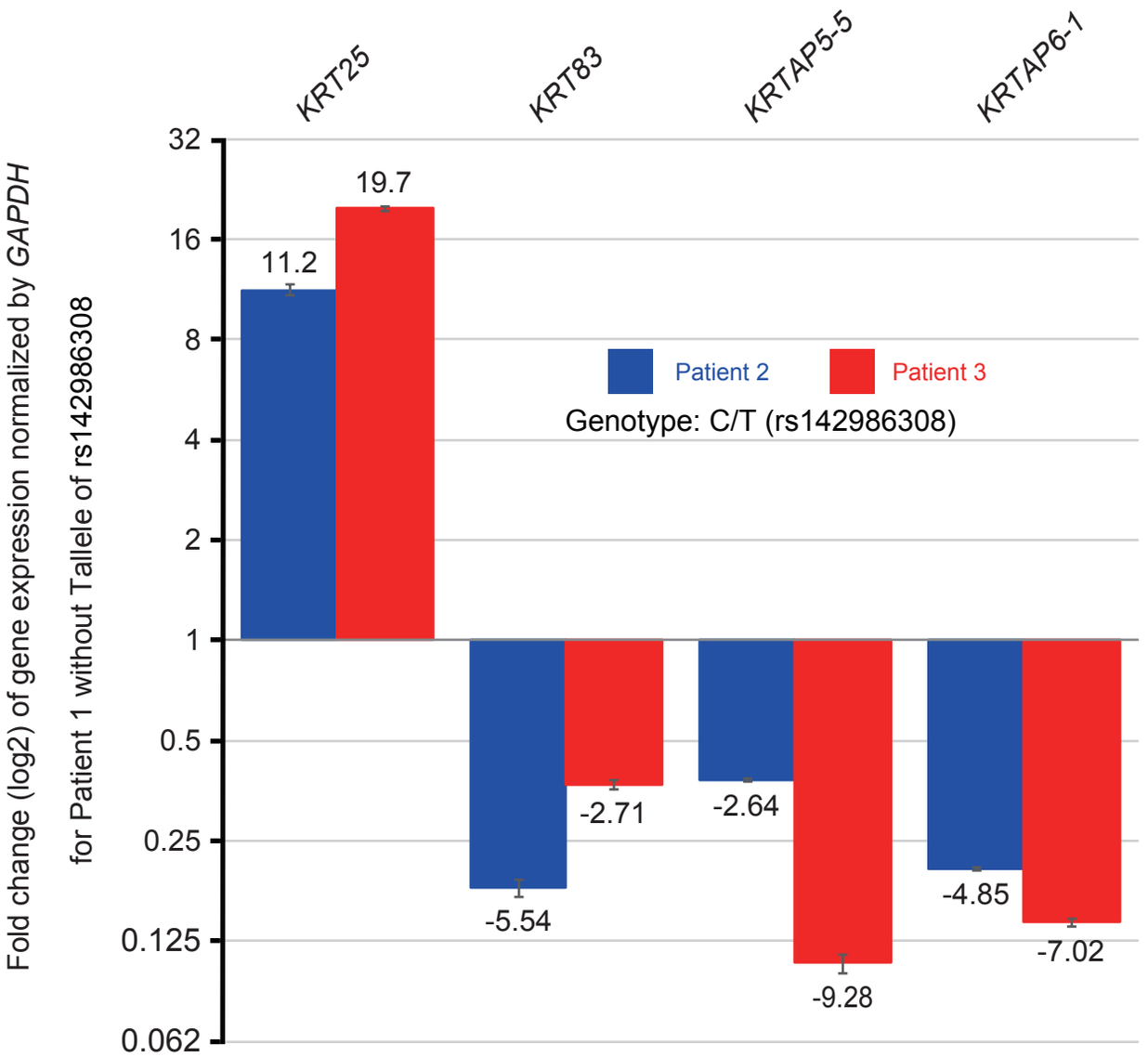

Supplementary Fig. 27. Validation of up or down regulated gene expression for 4 selected genes. Hair follicles of AA patients were subjected to expression analysis by qPCR and a comparative CT method. Bars reflect 95% confidence intervals. Fold change values were normalized to hair follicle of an AA patient without T allele of rs142986308 as a calibrator, thus the fold change value of the calibrator was always one.

Case

Control

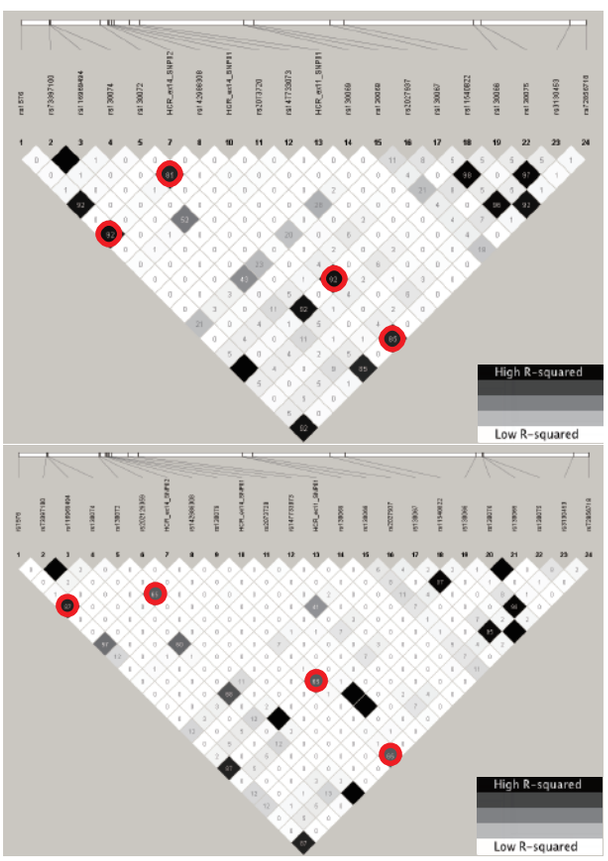

Supplementary Fig. 28. Pair-wise LD between 24 variants with amino acid substitution in *CCHCR1*.

LD was evaluated using R-squared values. Red square shows SNV pairs demonstrating strong LD with rs142986308.